CFD Simulation of Fire Spreading in a Residential Building: The Effect of Implementing Phase Changing Materials

Dionysios I. Kolaitis[1*], Eleni K. Asimakopoulou[2], Maria A. Founti[3]

[1, 2, 3] Laboratory of Heteregeneous Mixtures and Combustion Systems, Thermal Engineering Section, School of Mechanical Engineering, National Technical University of Athens, Greece.

Abstract
A CFD simulation is performed in a two-storey residential building subjected to a typical domestic kitchen fire. The building is constructed using a structural steel frame configuration combined with dry-wall systems. The addition of Phase Changing Materials (PCM) into the gypsum plasterboard structure is known to improve the building's energy utilization; the adverse impact of released PCM vapours on fire characteristics is investigated. Numerical predictions of the temporal evolution of gas velocity, gas and wall temperatures, toxic gas concentrations and smoke movement are obtained, thus allowing the visualization of the developing flow-field, the assessment of the fire resistance of the building elements, as well as the risk assessment for the tenants of the building in the event of a fire.

Introduction

Fire is one of the most complex phenomena considered in combustion science, since it embraces nearly all the effects found in subsonic chemically reacting flows. Fluid dynamics, combustion, chemical kinetics, radiation and multi-phase flow effects are linked together to provide an extremely complex physical and chemical phenomenon. It is this complexity that delayed the development of fire research as a science until the 1950s. Fires are associated with a large range of hazards to humans, property and the environment. Amongst the variety of incidents of uncontrollable fires, unwanted fires in enclosures are the most frequently encountered [1]. In building fires, the confined space controls the air supply and thermal environment of the fire, which affect the spread, growth, maximum burning rate and duration of the fire. Fire safety regulations have a major impact on the overall design of buildings with regard to layout, aesthetics, function and cost.

According to the National Fire Protection Association, there were 1,451,500 fires in the U.S.A. during the year 2008; 84% of all fire fatalities occurred in homes, i.e. one- and two-family dwellings and apartments [2]. The most important areas of fire origin in residential buildings are the kitchen (34%), the bedroom (12%) and the living room (6%) [3]. Cooking fires are often the result of the ignition of loose clothing or other nearby flammable materials from unattended cooking where grease or oil ignites. In 2003, there were 118,700 reported cooking-related home structure fires in the U.S.A., which resulted in 250 fatalities, 3880 injuries and $512 million in direct property damage [4, 5]. In Europe, 2.0 - 2.5 million fires are reported per year, resulting n 20,000-25,000 fire deaths and 250,000-500,000 fire injuries per year. About 80% of the fatalities occur in private homes [6].

In recent years, a variety of numerical tools has been developed to enable the prediction of fire growth within enclosures. Computational Fluid Dynamics (CFD) tools allow the numerical solution of the fundamental equations describing the transfer of mass, momentum and energy in an enclosure fire environment. These tools have been successfully used in a variety of fire safety areas, such as fire protection engineering (e.g. prediction and visualization of fire and smoke movement), building architectural design (prediction of fire behaviour to estimate the optimal place for fire exits or sprinkler placement and operation), fire safety strategy for a building (e.g. prediction of smoke flow patterns to estimate the optimal design of smoke control systems), accident investigation, building re-design etc. The role of CFD tools in fire research is steadily increasing as the models become progressively robust and sophisticated and validation studies make them more reliable. The CFD approach is considered to be fundamental to the future development of fire models, which can provide the basis for performance-based fire safety regulations.

In this context, the use of CFD tools is necessary to extend beyond simplified geometrical configurations in order to ascertain their applicability in real building fires. However, most of the available studies focus mainly in single-room or two-room simulations [7, 8]. Scarce reports are available in the open literature regarding multi-room compartment fire simulations; they mainly focus on the investigation of accidental fires [9]. A round-robin study performed recently has revealed the difficulties associated with modelling fire dynamics in complex fire scenarios using CFD tools, suggesting that the respective accuracy of fire growth predictions is still generally poor [10].

Specific Objectives

The main scope of the present study is to investigate the ability of currently available state-of-the-art CFD tools to effectively simulate the turbulent, multi-component and reactive flow-field developing in a full-scale two-storey residential house during a fire, taking into account detailed material properties. The fire resistance characteristics of a structural steel frame configuration combined with dry-wall systems is investigated. A parametric study, regarding the addition of Phase Changing Materials (PCM) in gypsum plasterboards is performed, examining the impact of PCM addition on fire characteristics.

Residential Building Geometrical Setup

The modelled two-storey, 152 m², residential house represents a typical Greek family two-storey dwelling, Fig. 1, with a typical residential arrangement plan (ground floor: kitchen, office and living room, first floor: master and auxiliary bedroom). The building is constructed using a load-bearing steel frame combined with dry wall system (multi layered plasterboard assemblies), in accordance with earthquake, fire-resistance, thermal and sound insulation requirements. The external walls of the house are multi-layered, consisting of (from the interior to the exterior) two 12.5 mm plasterboards, a 182.5 mm void (allowing space for the steel frame and plumbing), a 12.5 mm plasterboard, a layer of 80 mm Rockwool, a 12.5 mm Cementboard and a final layer of 50 mm EPS polystyrene. The internal walls consist of two 12.5 mm plasterboards, a layer of 80 mm Rockwool and two 12.5 mm plasterboards. The thermo-physical properties of the construction and furniture materials used in the building were obtained from the open literature [11, 12, 13].
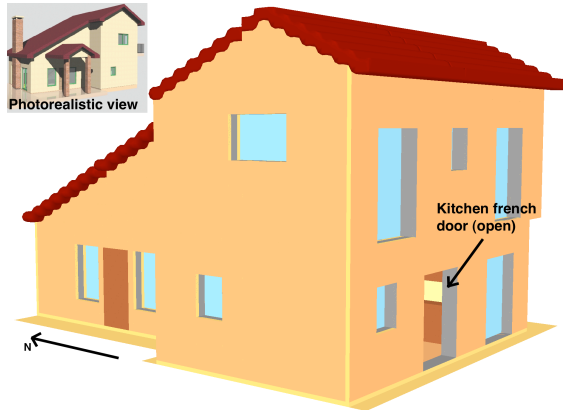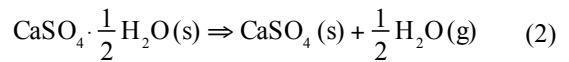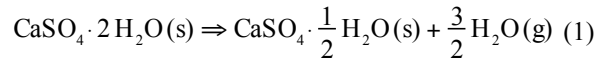

Fig. 1. General layout of the simulated building.

Fire Behaviour of Gypsum Plasterboards

Gypsum plasterboards are widely used in the building industry for a variety of applications as an aesthetically pleasing, easily applied and mechanically enduring facing material for walls and ceilings. In the context of building fire safety, gypsum plasterboards are capable of decelerating the penetration of fire through walls and floors, due to the endothermic gypsum dehydration process occurring in high temperatures. When a gypsum plasterboard is subjected to a high temperature environment, water molecules bound in its crystal lattice are released and transferred through the board, absorbing energy and thus reducing the mean wall temperature. This process is known to improve the global fire resistance of the building and it is suggested to enhance the safety margins of the building, by allowing longer evacuation times [12].

A typical gypsum plasterboard consists mainly of gypsum combined with 21% by weight chemically bound water, known as calcium sulphate dehydrate ($CaSO_4 \cdot 2H_2O$). In addition, gypsum usually contains a small amount of absorbed water, as well as calcium carbonate ($CaSO_4$). When gypsum is heated above 90°C the chemically bound water dissociates from the crystal lattice and evaporates. This process, known as gypsum "dehydration", occurs in the temperature region between 90°C and 250°C, depending on the heating rate and requires the absorption of a large amount of heat [14].

The dissociation of the chemical bound water takes place in two stages. In the first stage (Equation 1), the calcium sulphate dihydrate loses 75% of its water, thus forming calcium sulphate hemi-hydrate ($CaSO_4 \cdot \frac{1}{2}H_2O$). If gypsum is heated further, a second reaction occurs (Equation 2), where the calcium sulphate hemi-hydrate loses the remaining water to form calcium sulphate anhydrate ($CaSO_4$). Both reactions are endothermic and absorb a large amount of energy.

$$CaSO_4 \cdot 2H_2O(s) \Rightarrow CaSO_4 \cdot \frac{1}{2}H_2O(s) + \frac{3}{2}H_2O(g) \quad (1)$$

$$CaSO_4 \cdot \frac{1}{2}H_2O(s) \Rightarrow CaSO_4(s) + \frac{1}{2}H_2O(g) \quad (2)$$

The physical properties of gypsum are varying with increasing temperatures, due to the occurring dehydration reactions. The utilization of temperature-dependent physical properties is known to yield more accurate results in heat transfer simulations of gypsum plasterboards, compared to mean values [15] and therefore, temperature-dependent values for thermal conductivity and specific heat were used in the simulations.

Both gypsum dehydration and water vapour diffusion have a strong impact on the heat transfer characteristics of gypsum plasterboards exposed to fire conditions. In order to implement these effects in the utilized CFD code, a detailed solution of the respective heat and mass transfer equations across the width of the gypsum plasterboard would be required; since the computational cost of such simulations is currently prohibitive, an alternative methodology has been followed. The effects of the aforementioned transport phenomena have been incorporated into the specific heat values, thus constructing an "effective" specific heat temperature profile, which has been utilized in the simulations.

$$c_{P,eff}(T) = c_{P,s}(T) + \sum_{i=1}^{2} f_i c_{P,i}(T) \quad (3)$$

The effective specific heat of the gypsum plasterboards was defined using Equation (3). $c_{P,s}$ represents the "original" specific heat value of gypsum plasterboards, whereas the $c_{P,i}$ values correspond to additional "effective" specific heats owed to the endothermic dehydration reactions occurring in elevated temperatures; the integral of each additional specific heat is equal to the energy absorbed in the respective reaction. The $c_{P,i}$ values have been estimated using Differential Scanning Calorimetry (DSC) measurements performed in actual gypsum plasterboards. The f_i terms

correspond to mass transfer correction factors, which take into account the effects of vapour migration in the gypsum porous structure. The, in-house developed, HETRAN simulation tool [14], which models the simultaneous heat and mass transfer inside porous materials, has been used to define the values of the mass transfer correction factors; their were found to be equal to 1.45, corresponding to a 45% increase of the total dehydration energy.

Fire Behaviour of Phase Changing Materials

The incorporation of Phase Changing Materials (PCM) into building materials has been investigated for more than three decades as a way of increasing the thermal mass of building structure elements [16]. This innovative technique takes advantage of the latent heat of the PCM during the solid-to-liquid phase change to stabilize the temperature of the material and reduce the heat losses/gains from the building to the environment [17]. PCM can be incorporated in concrete, gypsum plasterboards, plaster and other building materials [18, 19]. The solid-liquid phase change occurs in the typical temperature range found indoors (20-26°C) is favourable for building energy consumption purposes. However, in the unlikely event of a fire, building materials may be exposed to substantially higher temperatures, that may even reach 800°C. In this case, paraffinic-based PCMs are expected to evaporate, since the boiling point of most paraffins lies below 350°C. As a result, in the case the PCM encapsulation shell is broken, the produced paraffin vapours may be released to the porous structure of the gypsum plasterboard and, through mass diffusion processes, emerge to the main combustion region. In this case, paraffin vapours are expected to ignite, thus adversely affecting the building's fire resistance characteristics. The impact of this effect, in the case of a typical domestic fire, is investigated in the current study.

The thermal response of a commercial gypsum plasterboard with encapsulated PCMs has been estimated by performing Differential Scanning Calorimetry (DSC) tests at high heating rates (40 K/min and 80 K/min). The melting energy of the PCM used in the plasterboard was found to correspond to that of octadecane. As a result, the octadecane liquid-to-vapour phase change (Equation 4) was also implemented in the code, in order to effectively simulate the fire behaviour of the PCM-enriched gypsum plasterboard. The respective Arrhenius parameter values, used in the simulations, are given in Table 1.

$$C_{13}H_{38}(l) \rightarrow C_{13}H_{38}(g) \qquad (4)$$
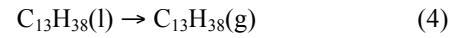
Fire Behaviour of Wood

The selection of the proper physical properties and pyrolysis rate coefficients for the combustible materials is a very challenging task; especially for the latter, values derived from small and large-scale experiments may exhibit differences of several orders of magnitude [20]. The simulated building was assumed to be equipped mainly with wooden furniture. A single step Arrhenius reaction was used to model the thermal decomposition of wood; the kinetic and thermal parameters used in the simulations were found in the literature [11]. The combustible gases produced by wood pyrolysis were described by the collective chemical species $C_{3.4}H_{6.2}O_{2.5}$ [21].

The FDS Code

The Fire Dynamics Simulator (FDS) code, version 5.5.3, was used to simulate the turbulent, multi-component and reactive flow-field developing inside the building. The FDS code is a CFD tool capable of studying fundamental fire dynamics and combustion, aimed at solving practical fire problems in fire protection engineering [22]. The FDS code solves numerically a form of the Navier-Stokes equations appropriate for low-speed, thermally driven flows; with an emphasis on smoke production and heat transfer from fires. The core algorithm is an explicit predictor-corrector scheme that is second order accurate in space and time. Turbulence is treated by using the Large Eddy Simulation (LES) approach. The subgrid-scale turbulence is simulated using the Smagorinsky model, utilizing a Smagorinsky constant value of 0.2. The numerical time-step is continuously adjusted in order to satisfy the CFL criterion. The partial derivatives of the conservation equations of mass, momentum and energy are approximated as finite differences and the solution is updated in time on a three-dimensional, Cartesian grid. Thermal radiation is simulated using the finite volume methodology on the fluid flow grid.

Table 1: Utilized kinetic parameters for the two-step gypsum dehydration and PCM release processes.

Reaction	$CaSO_4 \cdot 2H_2O \rightarrow CaSO_4 \cdot \frac{1}{2}H_2O$	$CaSO_4 \cdot \frac{1}{2}H_2O \rightarrow CaSO_4$	$C_{13}H_{38}(l) \rightarrow C_{13}H_{38}(g)$
Pre-exponential factor A (s^{1})	1.353779	0.456201	0.00839
Activation energy E (kJ/kmol)	2.46×10^4	2.28×10^4	6.532×10^4
(Endothermic) Heat of reaction (kJ/kg)	345	115	207.11
Water yield (kg H_2O / kg mixture)	12.75 %	4.87 %	-
Fuel yield (kg fuel / kg mixture)	-	-	18 %
Residue yield (kg residue / kg mixture)	87.25 %	95.13 %	82 %

All solid surfaces are assigned thermal boundary conditions by taking into account information about the burning behaviour of the respective material.

Computational Grid and Boundary Conditions

The considered building is enclosed within a rectangular volume, measuring 12.8 m, 10.2 m and 8.3 m, in the x-, y- and z- directions respectively. The numerical grid used divided this volume into 773,765 cubic computational cells, each having a side of 0.1 m. Certain construction and decorative details were "roughly" approximated in order to limit the size of the computational grid required for the simulations. However, the house was completely furnished, following a standard residential configuration. At the beginning of the numerical simulation ($t = 0$ s), the entire computational domain (both indoors and outdoors) is assumed to be still (zero velocity), exhibiting a temperature of 20°C. The total simulation time was 15 min, in order to be able to capture with sufficient detail the most important characteristic stages of the developing fire, namely initiation, spreading and decay. The total CPU-time needed for the complete simulation was approximately 24 hours on a desktop PC (Core i7 2.66 GHz CPU, 6 GB RAM), using the "parallel" version of the FDS code.

Cooking equipment is the primary cause of reported home fires and home fire injuries in the U.S.A. [5]. In this study, the ignition source was assumed to be a typical cooking fire represented by a 0.2 m by 0.2 m "patch" located on the upper surface of the birch wood kitchen bench. A constant 300 kW fire was assumed to appear at $t = 0$ s; the fire power was selected according to relative suggestions in the literature regarding fires related to kitchen equipment and cooking vegetable oil [23].

The computational domain extended approximately 1.0 m outwards from each side of the house; therefore, airflow in the surrounding environment could be also simulated, thus allowing studying of the effects of open external doors or windows. In order to investigate the effect of the encapsulated PCM in the fire-spreading rate, two test cases have been considered; test case G1 corresponds to the utilization of "conventional" gypsum plasterboards, whereas test case G2 represents the gypsum plasterboard with encapsulated PCM configuration. In both test cases the southern French door (1.6 m x 2.2 m), located very close to the fire source, was considered to be fully open, thus providing large amounts of fresh air into the main combusting zone (well-ventilated fire). All the internal openings were considered to be fully open.

Results and Discussion

Predictions of the gas phase velocity for the G1 test case are depicted in Fig. 2 along with the position of the maximum heat release rate iso-surface (which corresponds to the location of the simulated frame front) for the 6th minute of the simulation. The strong buoyant upward flow over the fire region produces a hot layer on the kitchen roof, which expands horizontally until it reaches the end of the 1st floor's corridor. There, two large counter-rotating vortices are formed; the most intense is the one extending to the upper floor, whereas the other corresponds to a slow recirculation zone in the main living room area.
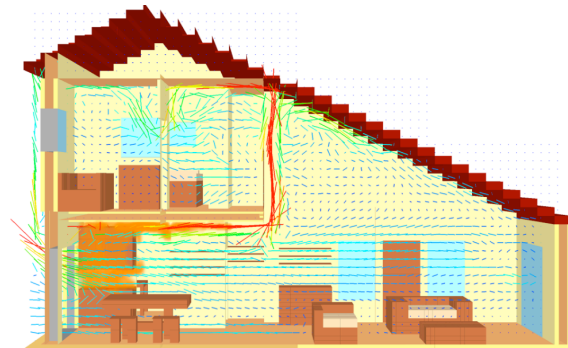

Fig. 2. Predictions of velocity vectors and flame surface 6 min after fire initiation (Test Case G1).

In Fig. 3, predictions of the wall surface temperature predictions in the kitchen are depicted for the 6th minute of the simulation. The side wall, which is directly exposed to the fire source, reaches high temperature levels (up to 1000°C) quite early in the simulation in both test cases.
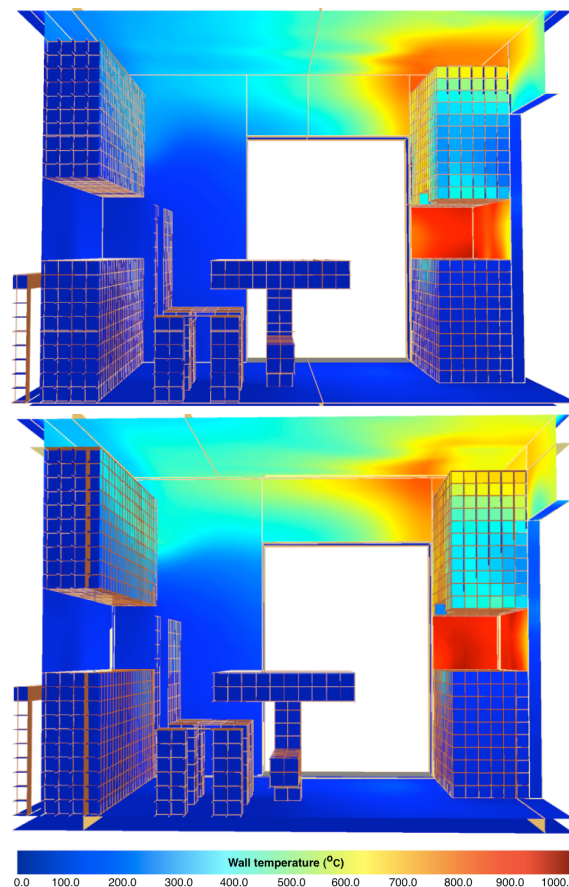

Fig. 3. Predictions of wall surface temperatures in the kitchen 6 min after fire initiation, for the G1 (top) and G2 (bottom) test cases.

Therefore, for test case G2 the paraffin in the encapsulated PCMs is expected to evaporate. As depicted in Fig. 3 wall temperatures in test case G2 reach higher values as the fire plume is affected from the vaporized paraffin fuel that contributes to its growth.

Gypsum plasterboards exposed to fire are considered to exhibit mechanical failure when cracks or openings are observed through the wall [24]; however, since cracking phenomena cannot be accurately simulated in the FDS code, alternative failure criteria had to be used. According to the Australian Standard AS1530.4, a plasterboard wall fails when the maximum temperature rise (above the ambient temperature) of the ambient facing side (unexposed side) exceeds $180^{o}C$ [25].

In Fig.4, wall surface temperature predictions across a section of the exterior kitchen wall, located near the fire for test cases G1 and G2, are depicted. Temperature predictions for the wall surface directly exposed to fire suggest that there is an advantage of test case G1, even though both curves are qualitatively similar; however, the "unexposed" side does not exceed the "limiting" temperature of $200^{o}C$ for neither case.
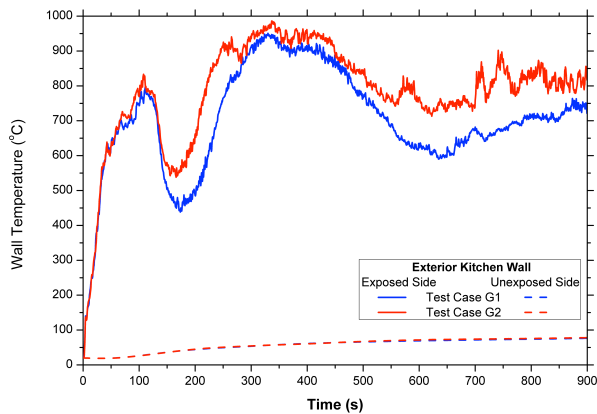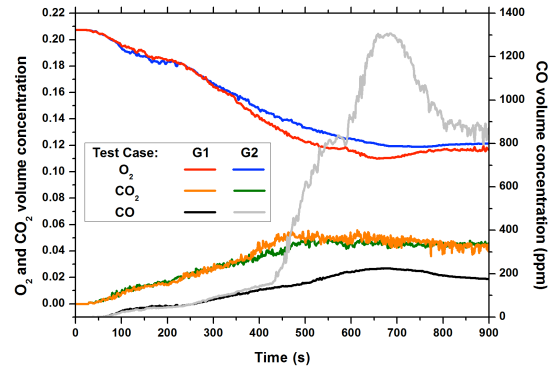

Fig. 4. Temporal evolution of the wall temperature of the exterior (south) kitchen wall, adjacent to the fire.

Tenability Limits

In order to evaluate life safety in fire conditions using a numerical modelling tool, quantitative tenability criteria are needed. An average person exposed for more than a few minutes to high levels of temperature and heat flux, is likely to suffer burns and die, either during or immediately after exposure, mainly due to hyperthermia. Respective values for the reported tolerance times in various temperatures are given in Table 2 [13]; tenability limits for incapacitation or death due to exposure to common combustion gaseous products, are also presented.

Predictions of O_2, CO_2 and CO volume concentrations in the middle of the kitchen are depicted in Fig. 5. The reported tenability limits for the CO_2 and CO concentrations are not exceeded for either test case. The values of CO_2 volume concentration in the case of PCM-enhanced gypsum plasterboards are slightly higher than in the case of conventional gypsum board. In test case G2, CO_2 concentration reaches a peak approximately 7.5 minutes after the fire initiation. In the

case of PCM-enhanced gypsum plasterboard, CO volume concentrations are higher than the respective values observed for the conventional gypsum board, due to the combustion of paraffin vapours. This remark indicates that combustion is largely incomplete in the case of test case G2. In the case of O_2 the observed values in both cases become lower than the reported maximum limiting value for incapacitation (13%), approximately 8 min after fire initiation.

Fig. 5. Temporal evolution of the O_2, CO_2 and CO volume concentrations in the middle of the kitchen (1.6m height).

The obtained gas temperature predictions in the kitchen room, at a characteristic height of 1.6m, are presented in Fig. 6. As expected, peak gas temperature values are higher in the case of PCM-enriched gypsum plasterboards, since when the evaporated paraffin is released in the combustion region, it is ignited, thus contributing in the fire load. During the first 8 minutes of the simulation the respective discrepancies are quite limited (the peak difference being $20^{o}C$). However, after the 8th minute the encapsulated PCM, in test case G2, starts to evaporate contributing to the fire load. The tenability limits for dry air temperature ($126^{o}C$) are reached in both test cases after the 5th minute of the simulation; however, only in test case G2 the time that the gas temperature remains above $180^{o}C$ is sufficient (4 min) to become hazardous.
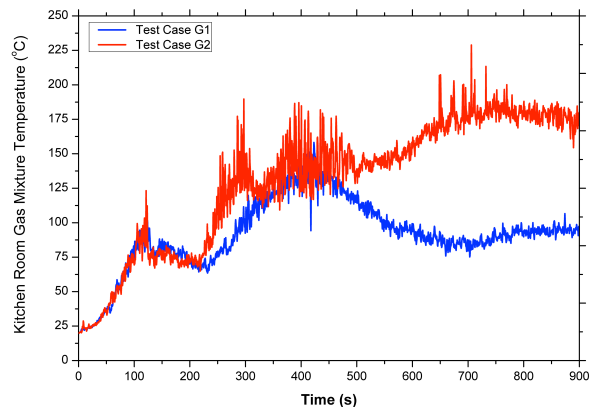
Fig. 6. Temporal evolution of the gas temperature in the middle of the kitchen, at a height of 1.6m.

Table 2: Reported tenability limits for 5-min exposure to common gaseous combustion products and tolerance time for exposure to warm air.

Gas Species	Incapacitation	Death
CO	6,000 - 8,000 ppm	12,000 - 16,000 ppm
O_2	10 - 13%	< 5%
CO_2	7 - 8%	> 10%

Air temperature (^{o}C)	Reported tolerance time (min)
126	7
180	4
205	3

Conclusions

A CFD tool has been used to simulate the thermal flow-field developing in a full-scale two-storey residential building during a fire. The considered building was constructed using a load-bearing steel frame combined with dry-wall systems. Detailed physical properties have been used to describe the thermal behaviour of the various building materials; the effects of gypsum dehydration were taken into account by utilizing temperature-dependent properties for the gypsum plasterboards.

Gas velocity and temperature predictions have been used to visualize the developing flow-field. Predicted wall temperatures allowed the assessment of the fire resistance behaviour of the investigated building using different construction materials. Also, gas temperature predictions allowed risk assessment for the tenants of the building.

The effect of PCM addition into the gypsum plasterboard structure has been investigated. When paraffinic PCM is heated, the encapsulation material may fail, thus allowing the produced PCM vapours to diffuse through the wall and be finally released to the fire region. In this case, the fire is intensified, thus increasing the predicted gas and wall temperatures, as well as the CO and CO_2 concentrations. Therefore, it becomes evident that microencapsulated PCM exhibiting adequate fire resistance characteristics need to be developed and manufactured.

The ability of currently available CFD tools to effectively simulate fire spreading in realistic residential fire scenarios has been demonstrated. However, due to the complexity of the occurring physico-chemical phenomena, further validation studies are needed to assess the quantitative accuracy of the obtained predictions.

Acknowledgments

References

[1] G. H. Yeoh and K. K. Yuen, Computational Fluid Dynamics in Fire Engineering, Elsevier, 2009.
[2] M. J. Karter, Fire losses in the United States during 2008, NFPA Report No FLX08, 2009.
[3] D. Madrzykowski and A. Hamins, Residential kitchen fire suppression research needs: Workshop Proceedings, NIST Special Publication 1066, Washington, U.S.A., 2007.
[5] M. Ahrens, Home fires involving cooking equipment, NFPA Report, U.S.A., 2010.
[6] Consumer fire safety: European statistics and potential fire safety measures, 431N8032/3.0, Netherlands Institute for Safety Nibra, 2009.
[7] Hasib, R., Kumar, R., Shashi and Kumar, S., Build. Environ. 42 (2007) 3149-3160.
[8] B. Merci and K. V. Maele, Fire Safety J. 43 (2008) 495-511.
[9] G. Rein, A. Bar-Ilan and C. Fernandez-Pello, J. Fire Prot. Eng. 16 (2006) 183-209.
[10] G. Rein, L. J. Torero, W. Jahn, J. Stern Gottfried, L. N. Ryder, S. Desanghere, M. Lazaro, F. Mowrer, A. Coles, D. Joyeux, D. Alvear, A. J. Capote, A. Jowrsey, C. Abecassis-Empis and P. Reszka, Fire Safety J. 44 (2009) 590-602.
[11] A. Matala, M.Sc. Thesis (2008), Faculty of Information and Natural Sciences, Helsinki University of Technology.
[12] C. Y. Wang and C. N. Ang, Constr. Build. Mater. 16 (2004) 505-515.
[13] P. J. DiNenno, D. Drysdale, C. L. Beyler, W. D. Walton, R. L. P. Cruster, J. R. Hall and J. M. Watts, (2002) SFPE Handbook for Fire Engineering, 3rd Edition, N.F.P.A., U.S.A.
[14] D. A. Kontogeorgos and M. A. Founti, Appl. Therm. Eng. 30 (2010) 1461-1469.
[15] D. A. Kontogeorgos, D. I. Kolaitis and M. A. Founti, Proc. of the 6th International Conf. on Heat Transfer, Fluid Mechanics and Thermodynamics (2008).
[16] F. Agyenim, N. Hewitt, P. Eames and M. Smyth, Renew. Sust. Energ. Rev. 14 (2010) 615-628.
[17] C. Voelker, O. Kornadt and M. Ostry, Energ. Buildings. 40 (2008) 937-944.
[18] I. Mandilaras and M. A. Founti, Effstock 2009, 11th Intern. Conf. on Therm. Energy Storage.
[19] M. Hunger, A. G. Entrop, I. Mandilaras, H. J. H. Brouwers and M. Founti, Cement Concrete Comp. 31 (2009) 731-743.
[20] S. Hostikka and K. B. McGrattan, Proc. of the 9th Int. Interflam Conf. (2001).
[21] J. S. Ritchie, D. K. Steckler, A. Hamins, G. T. Cleary, C. J. Yang and T. Kashiwagi, Proc. of the 5th Int. Sym. on Fire Safety Sc. (1997).
[22] K. McGrattan, S. Hostikka, J. Floyd, Fire Dynamics Simulator User's Guide, 2010.
[23] M. Luo and V. Beck, Fire Safety J. 23 (1994) 413-438.
[24] L. S. Manzello, G. R. Gann, R. S. Kukuck and B. D. Lenhert, Fire Mater. 31 (2007) 425-442.
[25] P. Clancy, Fire Tech. 38 (2002) 243-269.